

K.V. Korytchenko, O.V. Shypul, D. Samoilenko, I.S. Varshamova, A.A. Lisniak, S.V. Harbuz, K.M. Ostapov

NUMERICAL SIMULATION OF GAP LENGTH INFLUENCE ON ENERGY DEPOSITION IN SPARK DISCHARGE

The **aim** of the work is to study the influence of the length of the spark gap on energy input into the discharge channel during its gas-dynamic expansion. **Methodology.** The research is carried out by numerical modeling of the process of spark discharge development at variable values of the discharge gap length and at invariable other discharge conditions. The length of the gap was set in the range from 1 mm to 20 mm. The study was conducted using a numerical model of spark development, which takes into account the processes of nonstationary gas-dynamic expansion of the spark channel, the transient process in the electric circuit, nonequilibrium chemical processes, gas ionization, heat transfer and electrons thermal conductivity. The simulation was performed in atmospheric pressure nitrogen. The calculation was performed for various parameters of the RLC circuit, such as capacitance, inductance, resistance and voltage across the capacitor. **Results.** The study evaluates the influence of the spark length on the discharge current, the resistance of the spark channel, the energy deposited in the spark channel, and the distribution of thermodynamic parameters of the gas during the development of the spark discharge. It is confirmed that increasing the length of the gap increases the resistance of the spark. The deviation from the linear relationship between the deposited energy or the radiated energy and the length of the spark gap is estimated. **Scientific novelty.** A linear relationship between the gap length and the deposited energy is revealed when the total energy is above tens of Joules. Deviations from the linear dependence were detected in the discharge circuit when the total energy is below one of Joules. **Practical value.** The research results allow predicting the effect of the spark gap length on the energy input into the discharge channel under conditions of a slight change in the discharge current. In the conditions of essential change of amplitude of discharge current it is expedient to apply numerical researches for specification of changes in the energy deposited into a spark discharge. References 31, table 1, figures 13.

Key words: spark discharge, energy deposition, gap length influence.

Метою роботи є дослідження впливу довжини іскрового проміжку на введення енергії в розрядний канал під час його газодинамічного розширення. **Методика.** Дослідження здійснено шляхом чисельного моделювання процесу розвитку іскрового розряду за відмінних значень довжини розрядного проміжку та за незмінних інших умов розряду. Довжина проміжку задавалась в межах від 1 мм до 20 мм. Дослідження проведено з використанням чисельної моделі розвитку іскри, що враховує процеси нестационарного газодинамічного розширення іскрового каналу, перехідний процес в електричному колі, нерівноважні хімічні процеси, іонізацію газу, теплообмін випромінюванням та електронною теплопровідністю. Моделювання здійснювалось у азоті атмосферного тиску. Розрахунок проводився для різних параметрів RLC кола, таких як ємність, індуктивність, опір і напруга на ємності. **Результати.** В результаті дослідження оцінено вплив довжини іскрового на розрядний струм, опір іскрового каналу, енергію, що виділяється в іскровому каналі, та розподіл термодинамічних параметрів газу під час розвитку іскрового розряду. Підтверджено, що збільшення довжини проміжку збільшує опір іскри. Оцінено відхилення від лінійного співвідношення між енергією, що виділяється, або енергією, що випромінюється, та довжиною іскрового проміжку. **Наукова новизна.** У розрядному колі із накопиченою енергією понад десятки джоулів виявлено лінійну залежність між довжиною проміжку та енергією, що виділяється у ньому. У розрядному колі із накопиченою енергією до одного джоуля виявлено відхилення від лінійної залежності. **Практичне значення.** Результати досліджень дозволяють прогнозувати вплив довжини іскрового проміжку на введення енергії в розрядний канал в умовах незначної зміни розрядного струму. В умовах суттєвої зміни амплітуди розрядного струму доцільно застосовувати чисельні дослідження для уточнення змін в енергії, що вводиться в іскровий розряд. Бібл. 31, табл. 1, рис. 13.

Ключові слова: іскровий розряд, введення енергії, вплив довжини проміжку.

Introduction. Spark discharge is used in various devices where the length of the spark gap can vary in a wide range. The variation of the spark gap length results in the change of the spark channel resistance and it affects the discharge current. Finally, a change in the length of the spark gap leads to a change in the energy deposited in the spark discharge.

Resistance of an electrical conductor of a uniform cross section and conductivity is directly proportional to a length of the conductor. Therefore, an increase in the length of the electrical load leads to a linear rise in energy released in the load when a discharge current is the same. If the resistance of the discharge circuit significantly exceeds the resistance of the load, a change in the length of the load practically does not affect the discharge current. Thus, in a first approximation, there is a linear relationship between the load length and the energy

released in the load when the mentioned conditions take place. But the spark channel is an electrical conductor in which the cross section and conductivity change during the expansion of the spark channel. The discharge current determines the process of the spark channel expansion and, accordingly, affects the distribution of gas conductivity over the cross section of the spark channel. At the same time, the development of the discharge current depends on the resistance of the spark channel. As a result, the energy deposited into the spark channel deviates from a linear dependence on the spark gap length.

The study of the influence of the gap length on the deposited energy is important from a practical point of view. This is because spark energy affects the reliability of combustible mixtures ignition [1]. The energy of a spark discharge affects the detonation initiation process in

a detonation devices such as a pulse detonation engine and a pulse compression detonation gun [2-4]. The energy deposited into the spark channel has an impact on the period of the recovery of the dielectric strength of spark switches [5]. In nanoparticle generators, a change in the length of the discharge gap leads to a redistribution of the energy balance between the energy deposited in a gas-discharge channel and the energy loss at near-electrode regions [6]. This redistribution influences the efficiency of nanoparticle generation. The energy balance in the spark discharge also affects the energy efficiency of electrical discharge machining [7].

The energy deposition in a spark discharge with varied gap lengths was investigated experimentally in the work [8]. The authors measured the voltage across the spark gap with varied gap lengths to extract a voltage drop across the gas-discharge channel and a sum of cathode and anode voltage drops. So, it was assumed the voltage drop across the gas-discharge channel is directly proportional to the length of the spark gap. And the sum of cathode and anode voltage drops and electric field strength in the gas-discharge channel depend on a discharge time only. The voltage across the spark gap with varied gap lengths was measured at the different discharge time. Then the voltages were compared at the same discharge time to extract the voltage drop across the gas-discharge channel and the sum of cathode and anode voltage drops. Such comparisons were made at the different discharge time. Then the history of the voltage drop across the gas-discharge channel was found out. It allowed dividing the energy deposited in the spark gap into energy deposited in the spark channel and the energy deposited at the cathode and anode regions.

It has to note that an assumption of direct proportionality between the spark gap length and the energy deposited in the spark channel is correct if the discharge current does not change when the gap length is varied. But an increase in the spark gap length leads to a rise in the resistance of the discharge channel, and it decreases the discharge current, respectively. As a rule, the resistance of the spark channel is significantly lower than total impedance of the electric discharge circuit. Therefore, a change in spark resistance caused by a change in the gap length affects the discharge current slightly. Nevertheless, this effect occurs and it requires an evaluation.

An experimental study of the gap length influence on the energy deposition in a spark discharge was made in work [9]. The total energy of the spark discharge ranged from 25 to 45 mJ. The deposited energy was measured using a calorimetric technique. It was found out that an increase in the length of the discharge gap leads to growth in the energy deposited in the spark discharge. And it was evaluated that the increase in the deposited energy deviates from directly proportional dependence on the gap length. But measuring accuracy of the calorimetric technique did not allow updating the dependence of the deposited energy on the gap length.

The energy deposition in the spark discharge was investigated in works [2, 10] by damping factors comparison of a short circuit current with the discharge current when a gas-filled spark gap is used as a load. So,

the resistance of the electrical circuit was calculated from a damping factor of a short circuit current. A series connection of the spark gap with the electrical circuit leads to an increase in a resistance of the discharge circuit, and it influences on the damping factor of discharge current. Thus, the resistance calculated from the damping factor when spark gap is connected equals the sum of the circuit resistance and an average spark resistance. It allowed evaluating the average spark resistance then. And the deposited energy was found out by integration of discharge power over time.

It should be noted that the method applied in works [2, 10] does not give acceptable accuracy of the deposited energy measurement. It is caused by a wide range of the spark resistance change during the spark discharge evolution. Therefore, this method is not reasonable to use for studying the effect of the gap length on the deposited energy. Moreover, this method does not allow extracting the energy deposited in the gas-discharge channel from the energy deposited in the spark gap.

A gas-dynamic stage of spark development starts with a process of plasma channel contraction. The contraction usually happens when the duration of spark discharges exceeds a few hundreds of nanoseconds [11, 12]. Due to a significant growth in current density in the forming channel, the thermal ionization of the gas takes place in the channel, the gas becomes highly ionized, and the gas state exceeds an equilibrium one. The further development of the spark channel is accompanied by its gas-dynamic expansion. When duration of a spark discharge is over one microsecond and more, energy deposited in a gas-filled spark gap during the breakdown stage is typically lower than energy deposited during the stage of the gas-dynamic expansion. And the energy deposition at the expansion stage depends on the discharge current where a discharge electrical circuit influences the discharge current. So, we have studied the effect of the length of the gap on a spark discharges development when the energy deposition in the spark channel depends on the parameters of the electrical circuit.

There is a plurality of numerical models of spark development which adequately predict the processes occurring in the spark channel [13-18]. We used a numerical model of the spark channel expansion which was previously tested in a wide energy range [19-23].

The **aim** of the work is to study the influence of the length of the spark gap on energy input into the discharge channel during its gas-dynamic expansion.

Numerical model of spark channel expansion. It was assumed in the developed model that the expansion of the spark channel is determined by the following processes: non-stationary gas-dynamic expansion of the spark channel, a transient process in the electrical discharge circuit, nonequilibrium chemical processes, ionization of gas, radiation heat transfer and electron thermal conductivity. The process of collisions of electrons with atoms and molecules outside the thermally ionized spark channel was neglected because the electric field strength in the spark discharge during its expansion decreases to 100-1000 V/cm and lower [8]. The electrical conductivity was evaluated for a region of thermally

ionized gas where the degree of gas dissociation is high. Gray body radiation theory was used to take into account the radiative heat transfer in the high temperature gas and to simulate energy radiated from the high temperature spark channel [24]. Spectral radiative heat transfer in the low temperature gas was neglected due low power density. The nonequilibrium vibrational excitation of the gas in the shock wave was not considered. Molecular thermal conductivity was not taken into account because a value of such conductivity is significantly smaller than values of electron and radiative heat conductivities. The diffusion of atoms and molecules was not taken into account due to the high rates of mass transfer of the gas in the expanding channel. The scope of the model was limited by the condition that the magnetic pressure created by the discharge current is much less than the gas pressure.

Within the framework of the considered assumptions, the simulation of spark expansion was carried out by the system of equations

$$\frac{\partial}{\partial t} \begin{bmatrix} \rho \\ \rho u \\ \rho \varepsilon + \frac{\rho u^2}{2} \end{bmatrix} + \frac{1}{r} \frac{\partial}{\partial r} \begin{bmatrix} r \rho u \\ r(p + \rho u^2) \\ r \left(u \left(\rho \varepsilon + \frac{\rho u^2}{2} + p \right) + k_T \frac{dT}{dr} \right) \end{bmatrix} = \begin{bmatrix} 0 \\ \frac{p}{r} \\ \sigma E^2 - W_{em} \end{bmatrix}, \quad (1)$$

where ρ is the gas density; u is the velocity, p is the pressure, ε is the specific internal energy of the gas, k_T is the thermal conductivity, E is the electric field strength, σ is the electrical conductivity of the gas, W_{em} is the radiative loss, r is the radial coordinate, t is the time, T is the gas temperature.

The radiated energy was calculated using the expression

$$W_{em} = \sigma_{SB} T^4 / l_R, \quad (2)$$

where σ_{SB} is the Stefan–Boltzmann constant, l_R is the Rosseland mean free path.

The heat conductivity coefficient was calculated using the expression

$$k_T = k_e + k_{rad} = 2.65 \frac{T^{2.5}}{\ln \Lambda} + 5.33 \sigma_{SB} T^3 l_R, \quad (3)$$

where k_e is the electron heat conductivity coefficient, k_{rad} is the radiative heat conductivity coefficient, $\ln \Lambda$ is the Coulomb logarithm.

Transient electrical process was calculated by the equation

$$L \frac{di}{dt} + [R_c + R_{sp}] \cdot i + \frac{1}{C} \int_0^t i dt = 0, \quad (4)$$

where C is the capacitor capacitance, R_c is the resistance of a discharge circuit; L is the inductance of a discharge circuit, R_{sp} is resistance of the spark channel, i is a current.

Resistance R_{sp} was defined by the expression

$$R_{sp} = l_{sp} \int_0^Y 2\pi r \sigma dr, \quad (5)$$

where l_{sp} is the discharge gap length (channel); Y is maximum radius of the simulation domain, σ is an electrical conductivity.

The conductivity was calculated by equation

$$\sigma = 2.82 \cdot 10^{-4} \frac{n_e}{n_N \nu \sigma_{tr} + n_e \nu \sigma_{cul}}, \quad (6)$$

where n_e is electron number density; σ_{tr} is the transport cross-section of the elastic collisions of the electrons with the neutral plasma components; σ_{cul} is the Coulomb collision cross-section; n_N is the number density of neutral components; ν is a mean thermal velocity of electron.

The number density of neutral components was defined by equations of chemical reaction kinetics considering the reaction (Table 1) where forward rate constant k_f is expressed as

$$k_f = A_f T^{n_f} \exp\left(\frac{-E_{af}}{RT}\right). \quad (7)$$

Table 1

The coefficients of the rate constant of forward reaction and the activation energy [25]

| Reaction | A_f | n_f | E_{af} |
|-------------------------------------|-----------------------|-------|----------|
| $N_2 + M \leftrightarrow N + N + M$ | $8.508 \cdot 10^{25}$ | -2.25 | 225 |

Remark. M denotes the third particle. The values are expressed in calories, moles, cm^3 , and s.

The Saha equations with regard to the single and double ionization of gas with components of e , N , N^+ , N^{++} was applied to calculate the electron density n_e when the gas temperature exceeds 8000 K. It was assumed that plasma in the channel is quasi neutral too. A difference between temperature of electrons and temperature of atoms was estimated in the next section to evaluate a correctness of the local thermodynamic equilibrium approximation application.

The gas pressure was calculated using the expression

$$p = kT \sum n_c, \quad (8)$$

where n_c is a number density of all components (e , N , N^+ , N^{++} , N_2).

The simulation procedure is presented in Fig. 1.

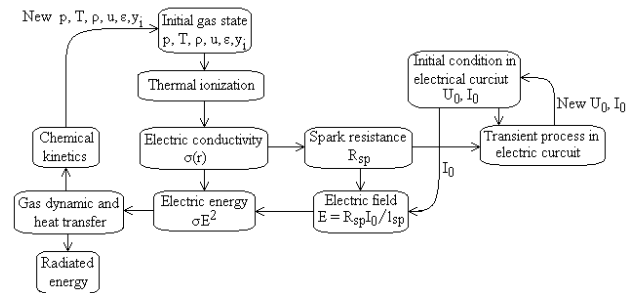


Fig. 1. Schematic of simulation procedure

Detail descriptions of the model and simulation procedure are presented in work [19].

The method of splitting by physical processes was applied to simulate gas-dynamic spark channel expansion combined with heat transfer and radiation, components concentration changing due to dissociation/association process, thermal gas ionization and transient process in electrical circuit.

The gradients of thermodynamic gas parameters are assumed to be absent for the discharge channel axis in a cylindrical symmetry. The computational area size was

prescribed in the manner of preventing disturbance from reaching the boundary. It is assumed that initial conditions have no gas dynamic perturbations in the entire computation region.

The model requires a circuit shorting to start simulating. The shorting of the discharge circuit occurs in a spark discharge as a result of the development of avalanche-spark or streamer-spark transition processes when the gap length is not extremely large. These processes are investigated, for example, in [5, 16]. As a result of these processes, a narrow channel with a radius of up to 0.1 mm is formed where a gas temperature of more than 10,000 K is reached, and the state of the gas approaches local thermodynamic equilibrium. Therefore, the energy was deposited into the channel of a small radius to rise the gas temperature from the initial one to 10,000 K. It is well known that when the capacitor discharge happens over the spark gap, the main part of the discharge energy is released during the high current pulses. Thus, the shorting energy was set in such a way that its value was significantly less than the total discharge energy. Therefore, a change in the conditions of the shorting energy deposition does not significantly influence the spark channel expansion because the further energy input into the spark is determined by the parameters of the discharge circuit. So, an energy was inputted initially in the simulated region with a radius of $r_0 = 50 \mu\text{m}$ during a time of $t = 10 \text{ ns}$ to form a narrow current-conducting channel. This energy was 2.8 mJ.

Results and discussion. A spark discharge in series RLC-circuit with various circuit parameters was investigated. The first circuit had follow parameters where the damping factor was $\zeta = 0.38$. A capacitance of $C = 0.2 \mu\text{F}$, an inductance of $L = 500 \text{ nH}$, a resistance of $R_c = 1.2 \Omega$ were applied. The charge voltage was $U_C = 3 \text{ kV}$. These circuit parameters correspond to the first simulation conditions. The second circuit had the following parameters where the damping factor was $\zeta = 0.11$. A capacitance of $C = 0.1 \mu\text{F}$, an inductance of $L = 2 \mu\text{H}$, a resistance of $R_c = 1 \Omega$ were applied. The charge voltage was $U_C = 30 \text{ kV}$. These circuit parameters correspond to the second simulation conditions. In both cases, a spark is ignited in molecular nitrogen with the initial gas temperature of $T_0 = 300 \text{ K}$ and the initial gas pressure of 0.1 MPa. A gap length was in a range from 1 mm to 20 mm.

The discharge currents at two electrical circuits with various spark gap lengths are shown in Fig. 2, 3. It is observed that an increase in the gap length led to a decrease in the amplitude of the discharge current at the both electrical circuits. But this effect is more pronounced at the first electrical circuit. So, the current amplitude at the first half cycle of the discharge decreased from 1111 A to 1010 A or by 10 % at the first circuit (Fig. 2) when the gap length is increased 3 times. Moreover, the current amplitude at the second half cycle of the discharge decreases by more than 45 %. The growth in the gap length to 6 mm caused a fall in the current amplitude at the first half cycle to 873 A or by 27 %.

The current amplitude at the first half cycle of the discharge decreased from 5669 A to 5471 A or by 3.65 %

only when the gap length is increased 10 times at the second circuit (Fig. 3). Moreover, the current amplitude reduction did not exceed 6.5 % in the second half cycle of the discharge. The current amplitude at the first half cycle of the discharge did not exceed 5261 A by the gap length of 20 mm.

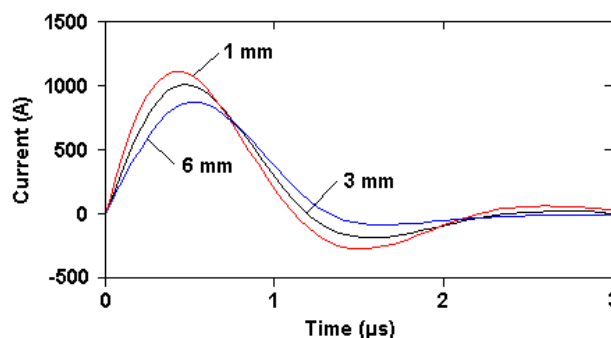


Fig. 2. The discharge current over time at the first electrical circuit with the gap length of 1 mm, 3 mm and 6 mm

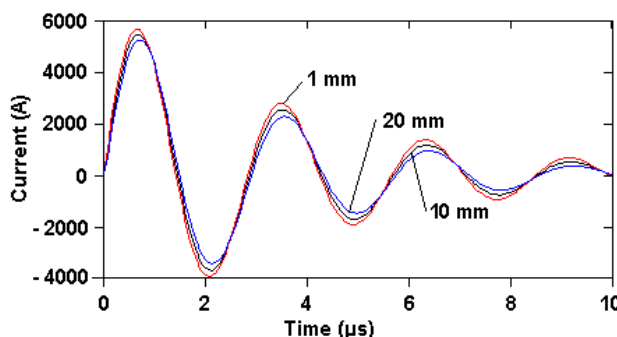


Fig. 3. The discharge current over time at the second circuit with a gap length of 1 mm, 10 mm and 20 mm

The dependences of the spark channel resistance on the discharge time at two electrical circuits with the various spark gap lengths are shown in Fig. 4, 5. In both cases the increased length of the discharge gap led to a rise in the resistance of the spark channel. The minimum value of the spark resistance in particular increases from 59 mΩ to 196 mΩ or 3.3 times at the first circuit (Fig. 4) when the gap length is enlarged three times. A six-fold increase in the length caused the minimum value rise to 449 mΩ or 7.6 times.

The minimum value of the spark resistance rises from 6.45 mΩ to 69 mΩ or 10.7 times at the second circuit (Fig. 5) when the gap length is enlarged ten times. And the minimum value grows to 147 mΩ or 22.8 times when the twenty-fold gap increase happens.

Thus, it was simulated that the minimum value of the spark resistance is nearly in direct proportion to the gap length.

The study of the gap length influence on the electric field strength in the spark channel at the calculated cases is presented in the Fig. 6, 7.

It is observed at the both circuits that a decrease in the field strength happens in 0.2–0.3 μs from the spark expansion start and the strength reduces to 1000 V/cm and lower. The effect of the gap length on the field strength is more pronounced at the first circuit (Fig. 6) than it effects at the second circuit (Fig. 7).

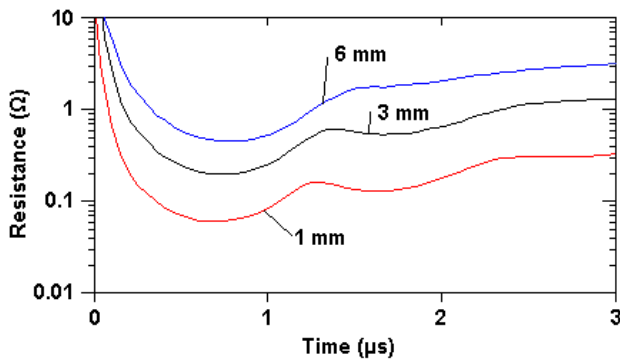


Fig. 4. The spark channel resistance over time at the first circuit with a gap length of 1 mm, 3 mm and 6 mm

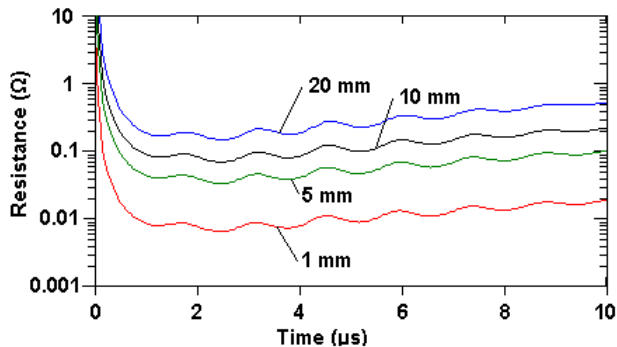


Fig. 5. The spark channel resistance over time at the second circuit with a gap length of 1 mm, 5 mm, 10 mm and 20 mm

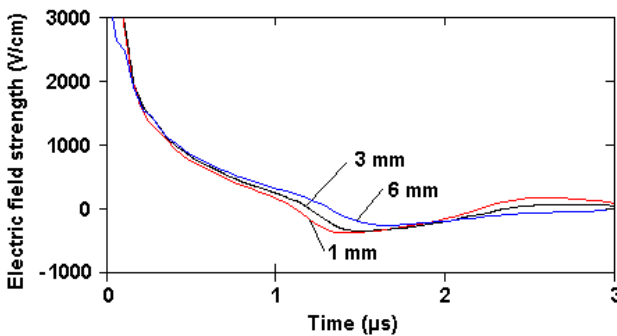


Fig. 6. The electric field strength over time at the first circuit with a gap length of 1 mm, 3 mm and 6 mm

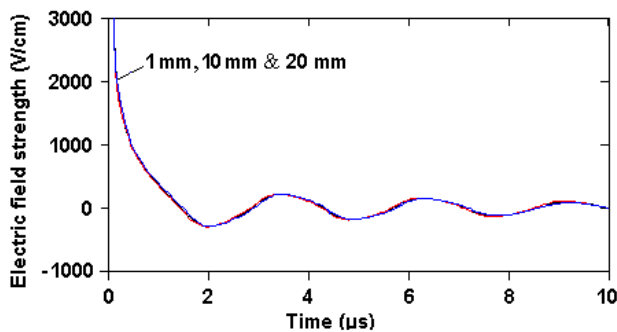


Fig. 7. The electric field strength over time at the second circuit with a gap length of 1 mm, 10 mm and 20 mm

The energy deposited in the spark channel over time at the calculated circuits with the various gap lengths is shown in Fig. 8, 9. We multiplied data of the deposited energy with a gap length of 1 mm by a number which equaled a ratio of the gap growth to find out the effect of the gap length on the deposited energy. It is observed that the deposited energy increases when the gap length rises.

Pulses of the discharge current cause an increase in the deposited energy. A main energy deposition happens during the first half cycle of the discharge. It is explained by a high discharge current and a high spark resistance during this period of the discharge development. The deviation of the energy growth from the directly proportional dependence on the gap length is observed at the both circuits (Fig. 8, 9). So, the three-fold increase in the deposited energy at the first circuit with the gap length of 1 mm differs by 11 % from the deposited energy at the case when the gap length was 3 mm (Fig. 8). Such an energy difference grows by 29 % when the gap length exceeds 6 mm. It should be noted that the Joule energy deposited in the resistance is directly proportional to the square of the discharge current. Therefore, it was previously expected that when the spark gap is increased from 1 mm to 6 mm at the first circuit, the deposited energy will decrease $1.27 \times 1.27 \approx 1.6$ times relative to 0.478 J (see Fig. 8) due to a decrease in the discharge current 1.27 times (see Fig. 2). So, the expected deposited energy was 0.298 J. But it was simulated that the deposited energy equals 0.371 J when the gap length is 6 mm. It occurs because a decrease in the discharge current causes an increase in the spark resistance that partially compensates for the drop in the deposited energy. For instance, when the gap length at the first circuit is increased 6 times, the minimum spark resistance increases not 6 times, but 7.6 times.

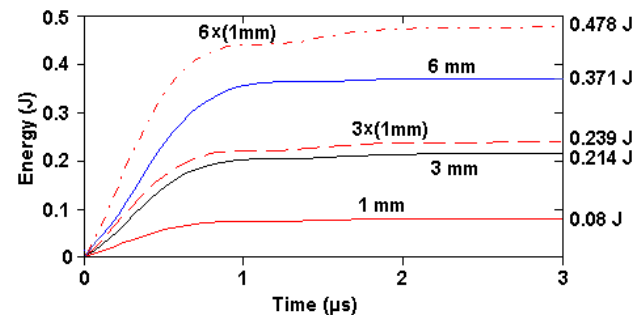


Fig. 8. The energy deposited in the spark channel over time at the first circuit with a gap length of 1 mm, 3 mm and 6 mm. The dotted line denotes the three-fold increase in the deposited energy at the first circuit with the gap length of 1 mm. The dot-and-dash line denotes the six-fold increase

The ten-fold increase in the deposited energy in the second circuit with the gap length of 1 mm differs by 6 % only from the deposited energy at the case when the gap length was 10 mm (Fig. 9). The deviation of the energy growth from the directly proportional dependence on the gap length at the first half cycle of the discharge did not exceed 3.6 % when the gap length was 10 mm. The difference in the deposited energy exceeds 13.2 % when the gap length equals 20 mm.

According to the simulation results we think that the energy deposited into the spark channel is directly proportional to the length of the spark gap as the first approximation. But when the minimum resistance of the spark channel and the resistance of the discharge circuit have the same order of magnitude and the damping factor is high, it is necessary to specify the deposited energy growth due to the gap length increase. A difference in the

discharge current can be used as a sign to specify the deposited energy.

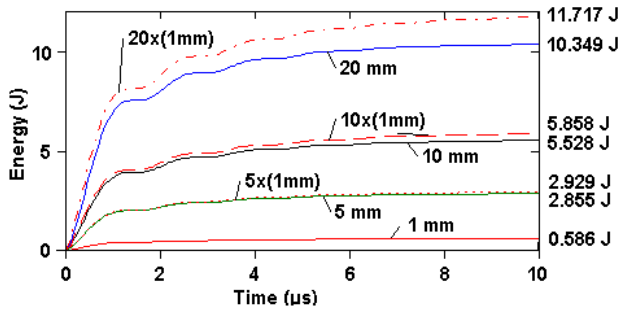


Fig. 9. The energy deposited in the spark channel over time at the second circuit with a gap length of 1 mm, 5 mm, 10 mm and 20 mm. The dashed line denotes the five-fold increase in the deposited energy at the second circuit with the gap length of 1 mm. The dotted line denotes the ten-fold increase, and the dot-and-dash line denotes the twenty-fold increase

Although extensive research has been carried out where the length of the discharge gap has been variable [6, 26], there is a problem to compare the calculated results with the experimental data. The reason for this is that a change in the gap length under constant gas pressure leads to a change in breakdown voltage. The increased breakdown voltage requires to rise the charge voltage of the discharge capacitor and, accordingly, to increase the total discharge energy. And growth in the total energy is accompanied by an increase in the energy deposited into the spark discharge. As a result, there are difficulties to separate the effect of the capacitor charge voltage from the effect of the gap length on the deposited energy.

Therefore, it was carried out a comparison of the calculated results with the results of experimental studies [9, 27], where the breakdown voltage did not change when the gap length is variable due to a regulation of the gas pressure p in the discharge medium.

It was assumed that the following condition take place

$$U_{br} = \text{const}, \quad \text{if } p \cdot l_{sp} = \text{const}, \quad (9)$$

where U_{br} is the breakdown voltage.

The results of experimental studies [9, 27] confirm that an increase in the length of the spark gap leads to a rise in the energy deposited into the gap. It is also confirmed that the change in the deposited energy deviates from a directly proportional dependence on the factor of change in the length of the gap. For example, it was found out in [9] that the thermal energy is 7 mJ at the experimental circuit when the gas pressure is 2 bar and the gap length is 1 mm. The thermal energy is about 12.5 mJ at such a circuit when the pressure is 1 bar and the length is 2 mm. Thus, there is a 1.78-fold increase in the deposited energy in the case of a two-fold increase in the length of the spark gap and a decrease in the pressure of the gas-discharge medium by a factor of two. To separate the effect of pressure from the effect of the gap length on the deposited energy, we use the data from [23], where it was found out that a 2-fold increase in gas pressure leads to an increase in the deposited energy by 10%. So, we have that a decrease in gas pressure from 2 bar to 1 bar by the gap length of 1 mm would lead to a

decrease in the deposited energy from 7 J to 6.3 mJ. As a result, we have that a two-fold increase in the gap length led to a 1.98-fold increase in the deposited energy.

The results of an experimental study of the effect of the gap length and the gas pressure on the realized energy are also presented in [27]. It should be noted that the total energy deposited into the discharge gap consists of the sum of the energy realized into the gas discharge channel and the energy released in the near electrode regions. The results of [27] allow us to separate these energy components. In particular, the energy released in the near-electrode regions corresponds to the total deposited energy when the spark gap length is about zero. According to the results of experimental studies, a close-to-linear relationship was found out between the gap length and the deposited energy. For example, it was measured [27] that the total deposited energy is 2.3 J at the investigated circuit with a spark gap of 1 mm and gas pressure of 1 bar. The following energy balance happens. The energy of 1.8 J is released in the near-electrode region, and the energy of 0.5 J is deposited in the spark channel. The total deposited energy equals 4 J at such a circuit when the gap length is 10 mm and the pressure is 0.1 bar where energy of 1.4 J is released in the near-electrode region, and energy of 2.6 J is released in the spark channel. According to the results of [23], an increase in pressure by a factor of 10 leads to an increase in the deposited energy by 70%. It follows that a decrease in pressure from 1 bar to 0.1 bar over a spark gap of 1 mm would lead to a decrease in the deposited energy from 0.5 J to 0.29 J.

Thus, an increase in the length of the gap by a factor of 10 led to an increase in the deposited energy 8.96 times. We have that the influence of the gap length, revealed by the results of numerical studies, is in satisfactory correlation with the experimental data.

Distribution of pressure, temperature and gas density along the radial coordinates at different time allow to evaluate an influence of the spark gap length on the discharge channel expansion (Fig. 10, 11).

There is a slight deviation of thermodynamic parameters with a change in the length of the spark gap at the first circuit (Fig. 10). This effect is caused by a reduction in the spark energy deposited per a unit of the gap length.

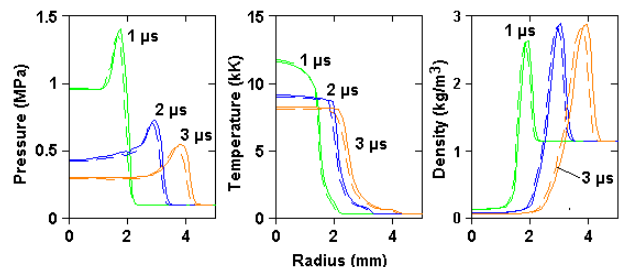


Fig. 10. Distribution of pressure, temperature and gas density along the radial coordinates at time of 1 μ s, 2 μ s and 3 μ s at the first circuit with a gap length of 1 mm (full lines) and 3 mm (dotted lines)

Negligible deviation of thermodynamic parameters was observed at the second circuit. Thus, it was difficult to show the difference in the Fig. 11.

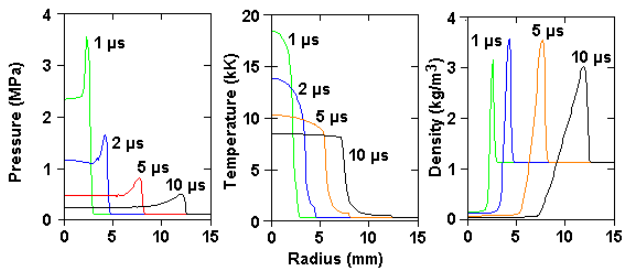


Fig. 11. Distribution of pressure, temperature and gas density along the radial coordinates at time of 1 μ s, 2 μ s and 3 μ s at the second circuit with a gap length of 1 mm and 10 mm

The simulated results of the spark evolution at the both considered cases correspond to the experimental data in general. So, the shock wave starts separating from the current conductive region (high-temperature region) in about 1 μ s from the spark expansion start. Also, the growth of the total energy of the discharge, which occurs during transition from the first to the second circuit, leads to an increase in the intensity of the generated shock wave. This qualitative comparison and the previous verification of the model give reason to consider that the obtained results are reliable.

Due to the visible difference in the temperature distribution at the first circuit, the effect of the gap length on the energy radiated by the spark discharge was estimated for this case. The results of the radiated energy versus time for the gap length of 1 mm, 3 mm and 6 mm are presented in Fig. 12.

It is observed that growth of the gap length leads to a rise in the radiated energy. A three-fold increase in the radiated energy at the first circuit with a gap length of 1 mm differs from the radiated energy at such a circuit with a length of 3 mm by 13 % (Fig. 12). Thus, we have a similar tendency of influence of the gap length on the radiated energy. But the influence on the radiated energy is slightly intensive than the influence on the deposited energy.

We should separately discuss the possible effect of changing the length of the discharge gap on the cathode and anode voltage drop and, accordingly, on the energy released in the spark. There are two contradicting results on the magnitude of the voltage drop in the near electrode regions in the spark discharge.

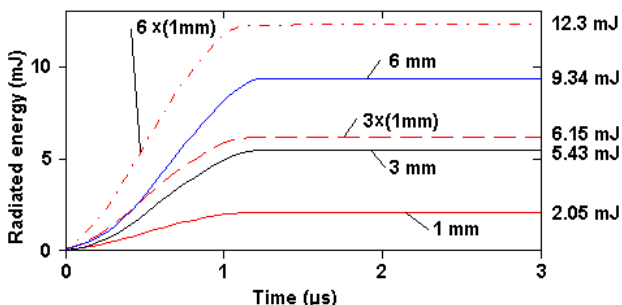


Fig. 12. Dependence of energy radiated by the spark discharge on time at the first circuit with a gap length of 1 mm and 3 mm.

The dotted line denotes three-fold increasing radiated energy when the gap length was 1 mm. The dot-and-dash line denotes the six-fold increase

According to the data of [28], the near-electrode voltage drop does not depend on the discharge current that

happens in the stationary arc discharge. And the voltage drop is about several volts. Since the voltage drop across the spark channel, as a rule, is several times higher than the mentioned near-electrode voltage drop, the influence of this factor on the balance of energy release in the spark can be negligible in this case. According to the experimental data of [29], the voltage drop in the near electrode regions changes during the spark evolution. And this voltage is comparable in magnitude with the voltage drop across the spark channel. It was assumed in [23] that an increased voltage drop in the near electrode regions is caused by an increased current density in the spark discharge. Since a change in the length of the discharge gap leads to a change in the discharge current and current density, the influence of the change in the voltage drop in the near electrode regions on the balance of energy release in the spark discharge can influence more strongly in this case. Therefore, this issue requires a separate study.

It has to discuss a local thermo-equilibrium approximation application to a region where gas temperature is above 8000 K. We use a two-temperature plasma model to evaluate a difference between temperature of electrons and temperature of atoms [30]. We assumed that the temperature of electrons is quasi-steady and plasma is neutral. The atomic gas was considered. The double ionization of gas was neglected. The follow systems of equations were solved [30, 31]:

$$n_e = \left[6.06 \cdot 10^{21} n_N \frac{Z_i}{Z_a} T_e^{1.5} \exp\left(-\frac{E_i}{kT_e}\right) \right]^{0.5}, \quad (10)$$

$$\frac{e^2 E^2}{m_e v_m^2} = \frac{3}{2} \delta k (T_e - T_i), \quad (11)$$

$$p = n_N k T_i + n_e k (T_e + T_i), \quad (12)$$

$$v_m = (\sigma_{tr} n_N + \sigma_{cul} n_e) \cdot v, \quad (13)$$

$$v = 6.71 \cdot 10^7 \cdot \sqrt{T_e}, \quad (14)$$

$$\sigma_{cul} = \frac{2.87 \cdot 10^{-14} \ln \Lambda}{T_e^2}, \quad (15)$$

$$\ln \Lambda = 7.47 + \frac{3}{2} \log(T_e) + \frac{1}{2} \log(n_e), \quad (16)$$

where T_e is temperature of electrons; T_i is temperature of atoms; Z_a and Z_i are partition functions; E_i is the ionization potential; e is electron charge; m_e is electron mass; v_m is the effective collision frequency for momentum transfer; δ is a fraction of energy transfer by a single collision of electron with atom ($\delta = 2m_e/m_a$, where m_a is a mass of atom); $\ln \Lambda$ is the Coulomb logarithm.

The system of equation (10) – (16) can be solved when the gas pressure and the electric field strength are known. The growth in the strength of the electric field causes the rise in the temperature difference that follows from equation (11). Thus, we use data of the strength histories (Fig. 6, 7) by local maximums of the strength curves.

It was found out that when $p = 1$ MPa, $E = 300$ V/cm and $T_i = 10 \dots 13$ kK, the temperature difference was varied in the range from 0.5 % to 5.5 % (Fig. 13,a). This condition corresponds to the first circuit at time of 0.7...1 μ s.

The temperature difference growth when the temperature of atoms decreases. So, it was found out that when $p = 0.3$ MPa, $E = 150$ V/cm and $T_i = 8 \dots 9$ kK, the temperature difference was varied in the range from 11 % to 19 % (Fig. 13,b). This condition corresponds to the first circuit at time of 2.5...3 μ s. But this difference cannot significantly influence on the simulated result because the main energy deposition stopped at about 1 μ s (Fig. 8).

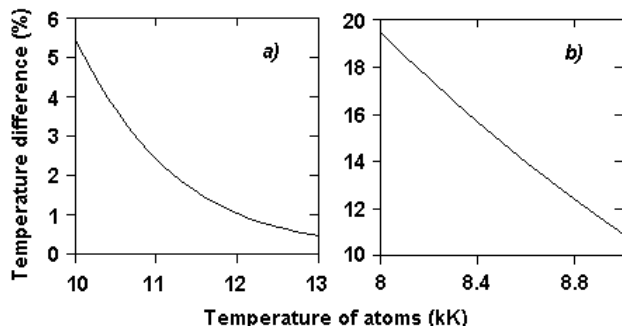


Fig. 13. Dependence of the temperature difference on the temperature of atoms when: a) $p = 1$ MPa, $E = 300$ V/cm and b) $p = 0.3$ MPa, $E = 150$ V/cm

The similar tendency for the temperature difference change happens at the second circuit. Taking into account the low value of the temperature difference, it allows us to assume that the local thermo-equilibrium approximation can be used in the numerical model.

Conclusions.

It was confirmed by the numerical study that the increase in the length of the discharge gap leads to growth in energy deposited into the spark discharge, a decrease in the amplitude of the discharge current and an increase in the resistance of the spark channel. But the change in the amplitude of the discharge current caused by the gap length variation depends on the discharge circuit parameters. We think the effect of the gap length on the discharge current enhances in case of a rise in the damping factor. So, it was observed that when the damping factor equaled $\zeta = 0.38$ at the simulated discharge circuit, three-fold increase in the gap length caused the decline in the current amplitude by 10 % at the first half cycle of the discharge. But when the damping factor equaled $\zeta = 0.11$, ten-fold increase in the gap length caused the decline in the current amplitude by 3.65 % only. The effect of the gap length on the electric field strength was more visible by the increased damping factor too. It was observed insignificant effect of the gap length on the spark channel expansion. It was found out that the minimum spark resistance, the deposited energy into the spark channel and the radiated energy are practically directly proportional to the spark gap length. But deviation from the direct proportionality rises when the minimum resistance of the spark channel and the resistance of the discharge circuit have the same order of magnitude and the damping factor is high. It was found out that the influence of the spark gap variation on the radiated energy is slightly intensive than the influence on the deposited energy.

Conflict of interests. The authors declare no conflicts of interest.

REFERENCES

1. Essmann S., Markus D., Grosshans H., Maas U. Experimental investigation of the stochastic early flame propagation after ignition by a low-energy electrical discharge. *Combustion and Flame*, 2020, vol. 211, pp. 44-53. doi: <https://doi.org/10.1016/j.combustflame.2019.09.021>.
2. Kamenskihs V., Ng H.D., Lee J.H.S. Measurement of critical energy for direct initiation of spherical detonations in stoichiometric high-pressure H₂-O₂ mixtures. *Combustion and Flame*, 2010, vol. 157, issue 9, pp. 1795-1799. doi: <https://doi.org/10.1016/j.combustflame.2010.02.014>.
3. Korytchenko K., Krivosheyev P., Dubinin D., Lisniak A., Afanasenko K., Harbuz S., Buskin O., Nikorchuk A., Tsebruk I. Experimental research into the influence of two-spark ignition on the deflagration to detonation transition process in a detonation tube. *Eastern-European Journal of Enterprise Technologies*, 2019, vol. 4, no. 5 (100), pp. 26-31. doi: <https://doi.org/10.15587/1729-4061.2019.175333>.
4. Zhang B., Bai C. Critical energy of direct detonation initiation in gaseous fuel-oxygen mixtures. *Safety Science*, 2013, vol. 53, pp. 153-159. doi: <https://doi.org/10.1016/j.ssci.2012.09.013>.
5. Zhang J., Markosyan A.H., Seeger M., Veldhuizen E.M., Heesch E.J.M., Ebert U. Numerical and experimental investigation of dielectric recovery in supercritical N₂. *Plasma Sources Science and Technology*, 2015, vol. 24, no. 2, pp. 025008. doi: <https://doi.org/10.1088/0963-0252/24/2/025008>.
6. Palomares J.M., Kohut A., Galbács G., Engeln R., Geretovszky Zs. A time-resolved imaging and electrical study on a high current atmospheric pressure spark discharge. *Journal of Applied Physics*, 2015, vol. 118, no. 23, pp. 233305. doi: <https://doi.org/10.1063/1.4937729>.
7. Gostimirovic M., Kovac P., Sekulic M., Skoric B. Influence of discharge energy on machining characteristics in EDM. *Journal of Mechanical Science and Technology*, 2012, vol. 26, no. 1, pp. 173-179. doi: <https://doi.org/10.1007/s12206-011-0922-x>.
8. Abramson I.S., Gegechkori N.M. Oscillographic research of spark discharge. *Journal of Experimental and Theoretical Physics*, 1951, vol. 21, no. 4, pp. 484-492.
9. Benito Parejo C., Michalski Q., Sotton J., Bellenoue M., Strozzi C. Characterization of Spark Ignition Energy Transfer by Optical and Non-Optical Diagnostics. *8th European Combustion Meeting*, 2017, ECM2017.0198.
10. Knystautas R., Lee J.H. On the effective energy for direct initiation of gaseous detonations. *Combustion and flame*, 1976, vol. 27, pp. 221-230. doi: [https://doi.org/10.1016/0010-2180\(76\)90025-0](https://doi.org/10.1016/0010-2180(76)90025-0).
11. Minesi N., Stepanyan S., Mariotto P., Stancu G-D., Laux C. On the arc transition mechanism in nanosecond air discharges, *AIAA Scitech 2019 Forum*, 2019, 2019-0463. doi: <https://doi.org/10.2514/6.2019-0463>.
12. Gegechkori N.M. Experimental studies of spark discharge channel. *Journal of Experimental and Theoretical Physics*, 1951, vol. 21, no. 4, pp. 493-506.
13. Tanaka Y., Michishita T., Uesugi Y. Hydrodynamic chemical non-equilibrium model of a pulsed arc discharge in dry air at atmospheric pressure. *Plasma Sources Science and Technology*, 2005, vol. 14, no. 1, pp. 134-154. doi: <https://doi.org/10.1088/0963-0252/14/1/016>.
14. Tanaka Y., Sakuta T. Modelling of a pulsed discharge in N₂ gas at atmospheric pressure, *Journal of Physics D: Applied Physics*, 1999, vol. 32, no. 24, pp. 3199-3207. doi: <https://doi.org/10.1088/0022-3727/32/24/316>.
15. Janda M., Machala Z., Niklová A., Martišovits V. The streamer-to-spark transition in a transient spark: a dc-driven nanosecond-pulsed discharge in atmospheric air. *Plasma Sources Science and Technology*, 2012, vol. 21, no. 4, p. 045006. doi: <https://doi.org/10.1088/0963-0252/21/4/045006>.

16. Marode E., Bastien F., Bakker M. A model of the streamer-induced spark formation based on neutral dynamics. *Journal of Applied Physics*, 1979, vol. 50, no. 1, p. 140-146. doi: <https://doi.org/10.1063/1.325697>.
17. Paxton A., Gardner R., Baker L. Lightning return stroke. A numerical calculation of the optical radiation. *Physics of Fluids*, 1986, vol. 29, no. 8, p. 2736. doi: <https://doi.org/10.1063/1.865514>.
18. Shneider M. Turbulent decay of after-spark channels. *Physics of Plasmas*, 2006, vol. 13, no. 7, p. 073501, doi: <https://doi.org/10.1063/1.2218492>.
19. Korytchenko K., Essmann S., Markus D., Maas U., Poklonskii Ye. Numerical and Experimental Investigation of the Channel Expansion of a Low-Energy Spark in the Air. *Combustion Science and Technology*, 2019, vol. 191, no. 12, pp. 2136-2161. doi: <https://doi.org/10.1080/00102202.2018.1548441>.
20. Korytchenko K., Markov V., Polyakov I., Slepuzhnikov E., Meleshchenko R. Validation of the numerical model of a spark channel expansion in a low-energy atmospheric pressure discharge. *Problems of Atomic Science and Technology*, 2018, vol. 4, pp. 144-146.
21. Korytchenko K., Poklonskiy E., Vinnikov D., Kudin D. Numerical simulation of gas-dynamic stage of spark discharge in oxygen. *Problems of Atomic Science and Technology*, 2013, vol. 4, pp. 155-160.
22. Korytchenko K.V., Poklonskii E.V., Krivosheev P.N. Model of the spark discharge initiation of detonation in a mixture of hydrogen with oxygen. *Russian Journal of Physical Chemistry B*, 2014, vol. 8, no. 5, pp. 692-700. doi: <https://doi.org/10.1134/S1990793114050169>.
23. Korytchenko K.V., Tomashevskiy R.S., Varshamova I.S., Meshkov D.V., Samoilenko D. Numerical investigation of energy deposition in spark discharge in adiabatically and isothermally compressed nitrogen. *Japanese Journal of Applied Physics*, 2020, vol. 59, no. SH, p. SHHC04. doi: <https://doi.org/10.35848/1347-4065/ab72cc>.
24. Zel'dovich Y.B., Raizer Yu. *Physics of shock waves and high-temperature hydrodynamic phenomena*. Dover Publications, Inc., Mineola, NY, 2002, 896 p.
25. Petersen E.L., Hanson R.K. Reduced kinetics mechanisms for ram accelerator combustion. *Journal of Propulsion and Power*, 1999, vol. 15, no. 4, pp. 591-600. doi: <https://doi.org/10.2514/2.5468>.
26. Belmouss M. Effect of electrode geometry on high energy spark discharges in air. *Thesis, Purdue University West Lafayette, Indiana*, 2015, 556.
27. Li X., Liu X., Zeng F., Yang H., Zhang Q. Study on Resistance and Energy Deposition of Spark Channel Under the Oscillatory Current Pulse. *IEEE Transactions on Plasma Science*, 2014, vol. 42, no. 9, pp. 2259-2265. doi: <https://doi.org/10.1109/tps.2014.2331346>.
28. Hemmi R., Yokomizu Y., Matsumura T. Anode-fall and cathode-fall voltages of air arc in atmosphere between silver electrodes. *Journal of Physics D: Applied Physics*, 2003, vol. 36, no. 9, pp. 1097-1106. doi: <https://doi.org/10.1088/0022-3727/36/9/307>.
29. Abramson I.S., Gegechkori N.M. Oscillographic research of spark discharge. *Journal of Experimental and Theoretical Physics*, 1951, vol. 21, no. 4, pp. 484-492.
30. Donskoi A.V., Goldfarb V.M., Klubnikin V.S., Dresvin S.V., Eckert H.U., Cheron T. *Physics and technology of low-temperature plasmas*. Iowa State University Press, 1977. 471 p.
31. Raizer Yu. *Gas discharge physics*. Springer-Verlag, Germany, 1991. 460 p.

Received 06.11.2020

Accepted 11.12.2020

Published 25.02.2021

K.V. Korytchenko¹, Doctor of Technical Science, Professor,
O.V. Shypul², Ph.D., Associate Professor,
D. Samoilenko³, Dr Hab. Inż.,
I.S. Varshamova¹, Senior Lecturer,
A.A. Lisniak⁴, Ph.D., Associate Professor,
S.V. Harbuz⁴, Ph.D.,
K.M. Ostapov⁴, Ph.D.,

¹ National Technical University «Kharkiv Polytechnic Institute»,
2, Kyrpychova Str., Kharkiv, 61002, Ukraine,

e-mail: korytchenko_kv@ukr.net, varshamova.i.s@gmail.com

² National Aerospace University «Kharkiv Aviation Institute»,

17, Chkalov Str., Kharkiv, Ukraine, 61070,

e-mail: o.shipul@khai.edu

³ Warsaw University of Technology,

Pl. Politechniki 1, 00-661 Warsaw, Poland,

e-mail: dmytro.samoilenko@pw.edu.pl

⁴ National University of Civil Defense of Ukraine,

94, Chernyshevska Str., Kharkiv, 61023, Ukraine,

e-mail: ptarr@nuczu.edu.ua, sgarbuz65@gmail.com,

ostapovk_90@ukr.net